Electronic Supplementary Material (ESI) for Physical Chemistry Chemical Physics.
This journal is © the Owner Societies 2019

Opportunities and challenges for electrochemistry in studying the electronic structure of nanocrystals

Michelle Weber, Sophia Westendorf , Björn Märker, Kai Braun, and Marcus Scheele

Supporting Information

Raman data

The samples used in Raman spectroscopy are prepared with the same dipcoating procedure as the samples in the main section, but on a silicon as the substrate.

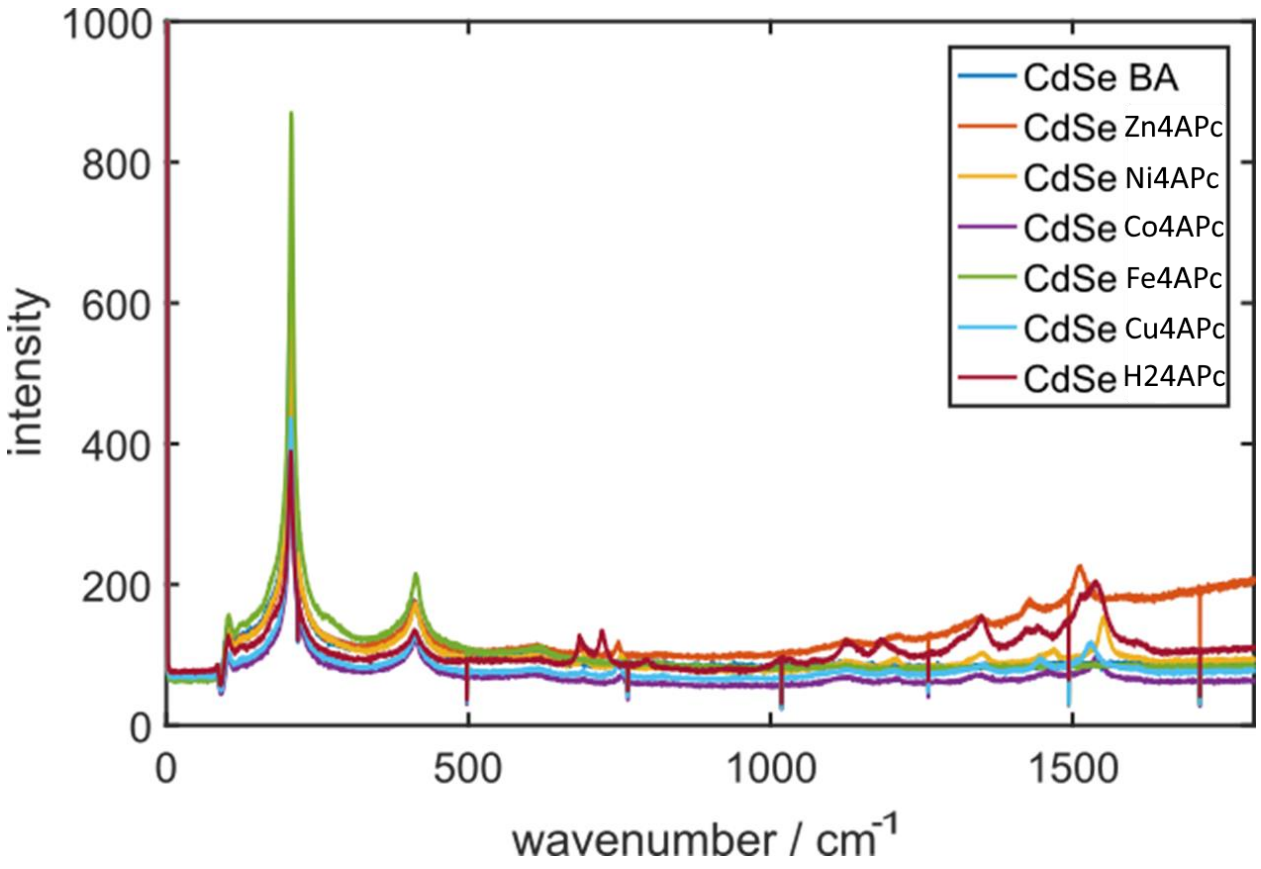

Figure S1: Raman spectra of all CdSe NC films used in this study cross-linked with various different molecules as indicated by the legend.

Table S1 summarizes the Raman peaks and assigns them to a characteristic vibration found in the literature:[1–5]

Table S1: Summary of Raman peaks observed in **Figure S1** and their assignment.

Peak #	CdSe + H_2Pc [cm^{-1}]	CdSe + ZnPc [cm^{-1}]	CdSe + NiPc [cm^{-1}]	CdSe + CuPc [cm^{-1}]	CdSe + CoPc [cm^{-1}]	description
1	207	207	207	207	207	CdSe
2	412	412	412	412	412	CdSe
3	684	685	692	690	691	bridging C-N-C sym def. pyrrole ring OP bend
4	722					macrocyle stretch / central ring twisting
5		750	752	748	753	central ring contraction
6	794					NH_2 wag
7	1019					C-H deformation & aryl C-C stretch
8	1024					C-H deformation & aryl C-C stretch
9		1127	1124	1123	1129	macrocyle stretch & C-H bend
11	1184					pyrrole ring breathing
12	1350	1349	1351	1355	1344	indole
13	1422	1429				indole
14	1442		1469	1446	1457	isoindole ring stretch
15	1516	1511		1530	1542	N-H in macrocyle ring stretch. benzene
16	1538	1581	1551	1608		macrocycle in plane stretch
17	1605		1611			NH_2 deformation

Discussion of the different types of uncertainties in the EMAS fits

The plot of the potential-dependent amplitude of the differential photovoltage in **Figure 6** in the main manuscript yields a curve with an s-shape. When fitting these curves with the equation (1), not all fits come out as ideal (**Figure S2a**). The less than ideal fits can be categorized into three different types of uncertainties:

A curve that shows error 1 (**Figure S2b**) shows a welldefined initial plateau region, from which $V_{PP,start}$ can be defined. At the end of the curve however, it only exhibits a very short plateau (sometimes consisting of only one data point), from which $V_{PP,end}$ can be defined. This is most likely due to the degradation of the sample at high potentials. A curve that shows error 2 (**Figure S2c**), does not form a plateau region in the end at all and is therefore particularly hard to fit. E_0 values resulting from a fit with error 2 should be treated with great caution. This curve shape most likely originates in inhomogeneous charging of the film. Error 3 (**Figure S2d**) results from a poor signal-to-noise ratio with some uncertainty in deriving the plateau potentials, and hence E_0.

The fits data sets analyzed in **Figure 6** are mostly of the ideal type depicted in **Figure S2a**.

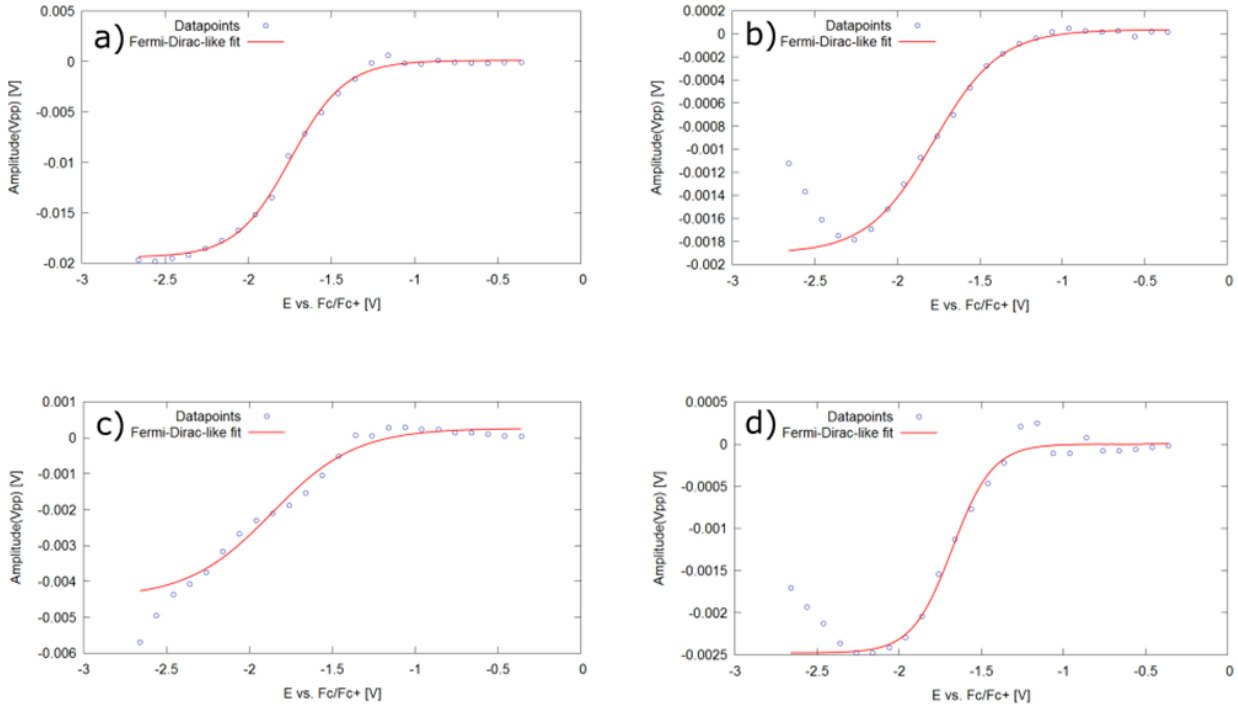

Figure S2: Fermi-Dirac fits of EMAS peaks recorded at a single wavelength and typical fit uncertainties.

Discussion of the phase of an EMAS signal

A lock-in amplifier is able to pick a signal of one specific frequency, lock this frequency and detect only the phase and amplitude of this signal. The amplitude is thereby recorded as a root mean square (RMS) value. For a sinusoidal curve as the one used in this work, the peak to peak amplitude of the signal can be calculated by the following transformation:

$$V_{pp} = RMS \cdot 2 \cdot \sqrt{2} \quad (1)$$

with V_{PP}, the magnitude of the detected signal. To determine whether it characterizes the absorption change caused by a bleach or an induced absorption, the phase of the signal is needed. Ideally, if increasing the potential in the reductive direction leads to an increase in absorption, the incoming and the outgoing signal are in phase and therefore have a phase shift of 0°. In the opposite scenario of a bleach, the incoming and outgoing signal should theoretically be phase-shifted by 180°. In reality, the current needs a finite time to reach the electrode and to polarize the NC film to invoke an absorption change. In addition, the detector has a finite response time. These factors lead to phase shifts that are not exactly 0° and 180°. In the analysis of the EMAS experiments in this work, it is assumed that all data points with a phase < ± 90° are an induced absorption and all data points with a phase > ± 90° are a bleach. **Figure S3** illustrates this. When looking at the spectrum of a sample at around the peak onset potential, it can be observed that before the peak onset potential (**Figure S3a**), the phase information is quite unstable and changes frequently between areas of phase > ± 90° (yellow, bleach) and < ± 90° (green, induced absorption,**Figure S3c**). After the sample passes the peak onset potential, the peaks in the spectrum become smoother and grow in magnitude (see **Figure S3b**). Also the phase stays well defined inside an area (see **Figure S3d**). From this phase analysis, peaks 1-4 in the main part of the manuscript are assigned as induced absorption (peaks 1,3) and bleach (2,4). The agreement with the work by Spittel et al. shows that the phase attribution made here is correct.[6]

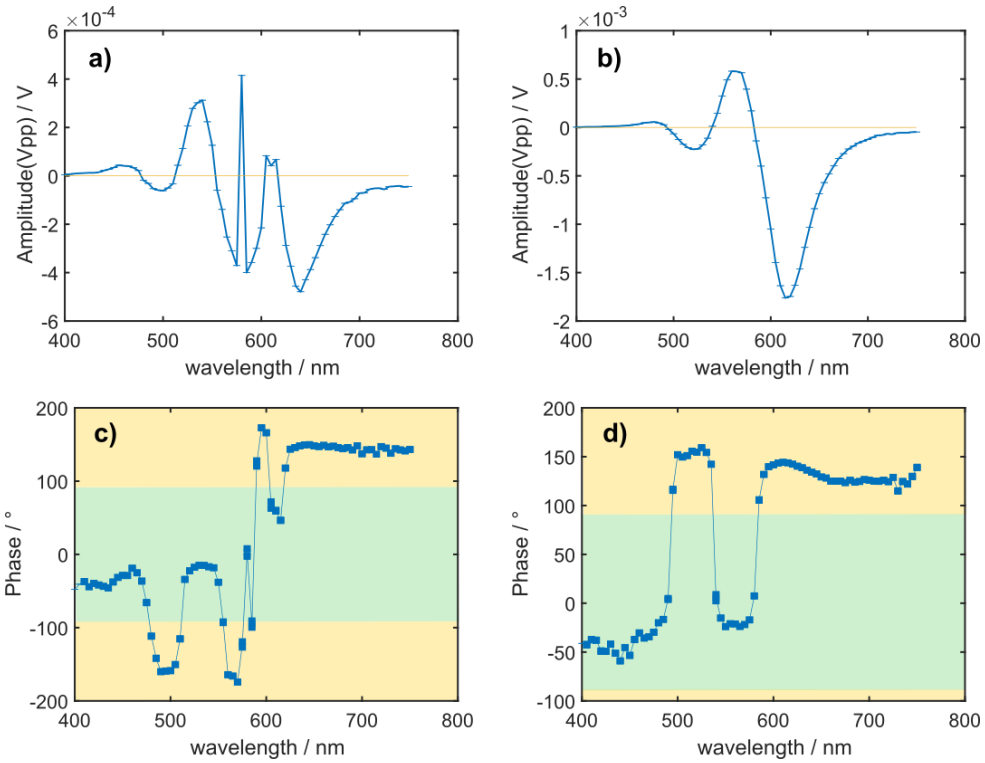

Figure S3: Typical EMAS amplitude and phase of a CdSe NC film. The upper row depicts the peak to peak amplitude in V for a potential of (a) -1.26 V vs. Fc/Fc^+ and (b) -1.36 V vs. Fc/Fc^+, similar to the data shown in **Figure 5a**. The bottom row depicts the respective phase of these datasets.

EMAS Spectrum of the bare FTO electrode

The FTO working electrode shows some absorption features between 400 and 750 nm. When an electrochemical potential is applied to the FTO, these absorption features broaden due to the quantum confined Stark effect.[7] This leads to some bleaches and induced absorptions in the same spectral region where the transitions of the CdSe NCs are also expected (see **Figure S4**). The peaks resulting from the CdSe NCs are one to two orders of magnitude stronger than the peaks originating from the FTO, so they can be clearly distinguished.

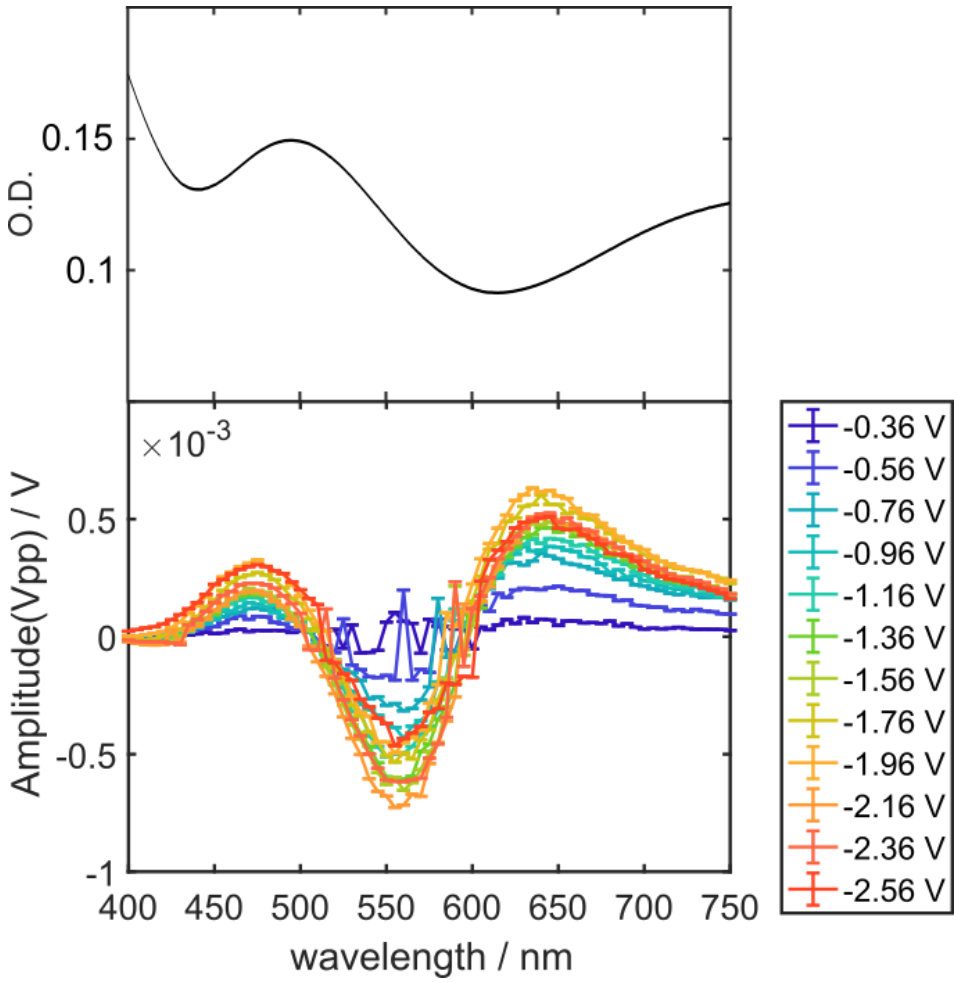

Figure S4: UV-Vis spectrum (above) and EMAS spectrum (below) of the uncoated FTO electrode.

References

1. A. Sivanesan and S.A. John, *Langmuir*, 2008, **24** (5), 2186.
2. K.S. Lokesh and A. Adriaens, *Dyes Pigm.*, 2013, **96** (1), 269.
3. C. Murray, N. Dozova, J.G. McCaffrey, S. FitzGerald, N. Shafizadeh and C. Crépin, *Phys. Chem. Chem. Phys.*, 2010, **12** (35), 10406.
4. G.X. Wang, M.S. Park, H.K. Liu, D. Wexler and J. Chen, *Appl. Phys. Lett.*, 2006, **88** (19), 193115.
5. M.H. Yükselici, A. Aşıkoğlu Bozkurt and B.C. Ömür, *Mater. Res. Bull.*, 2013, **48** (7), 2442.
6. D. Spittel, J. Poppe, C. Meerbach, C. Ziegler, S.G. Hickey and A. Eychmüller, *ACS Nano*, 2017, **11**(12), 12174.
7. D.A.B. Miller, D.S. Chemla, T.C. Damen, A.C. Gossard, W. Wiegmann, T.H. Wood and C.A. Burrus, *Phys. Rev. Lett.*, 1984, **53** (22), 2173.